

An X-Ray Induced Structural Transition in $\text{La}_{0.875}\text{Sr}_{0.125}\text{MnO}_3$

V. Kiryukhin, Y. J. Wang, F. C. Chou, M. A. Kastner, and R. J. Birgeneau

Department of Physics, Massachusetts Institute of Technology, Cambridge, MA 02139

(February 1, 2008)

We report a synchrotron x-ray scattering study of the magnetoresistive manganite $\text{La}_{0.875}\text{Sr}_{0.125}\text{MnO}_3$. At low temperatures, this material undergoes an x-ray induced structural transition at which charge ordering of Mn^{3+} and Mn^{4+} ions characteristic to the low-temperature state of this compound is destroyed. The transition is persistent but the charge-ordered state can be restored by heating above the charge-ordering transition temperature and subsequently cooling. The charge-ordering diffraction peaks, which are broadened at all temperatures, broaden more upon x-ray irradiation, indicating the finite correlation length of the charge-ordered state. Together with the recent reports on x-ray induced transitions in $\text{Pr}_{1-x}\text{Ca}_x\text{MnO}_3$, our results demonstrate that the photoinduced structural change is a common property of the charge-ordered perovskite manganites.

PACS numbers: 64.70.Kb, 71.30.+h, 72.80.Ga, 78.70.Ck

Perovskite manganites of the general formula $A_{1-x}\text{B}_x\text{MnO}_3$, where A and B are trivalent and divalent metals, respectively, have recently attracted considerable attention by virtue of their unusual magnetic and electronic properties [1]. These properties result from an intricate interrelationship between charge, spin, orbital and lattice degrees of freedom that are strongly coupled to each other. Manganite perovskites exhibit a variety of conducting and insulating phases possessing different types of magnetic ordering and structural distortion. Transitions between these phases can be induced by varying temperature, pressure, or magnetic field. In the latter case the celebrated phenomenon of “Colossal Magnetoresistance” is observed.

Recently, the manganite perovskite $\text{Pr}_{1-x}(\text{Ca},\text{Sr})_x\text{MnO}_3$ ($x = 0.3 - 0.5$) has been shown to undergo an unusual insulator-metal transition when it is exposed to an intense x-ray beam at low temperatures [2]-[5]. (Visible light does not induce the transition unless an external electric field is applied [6].) $\text{Pr}_{0.7}\text{Ca}_{0.3}\text{MnO}_3$ is a paramagnetic semiconductor at high temperatures, and a charge ordered (CO) antiferromagnetic insulator with a static superlattice of Mn^{3+} and Mn^{4+} ions below $\sim 200\text{K}$ [7,8]. Upon x-ray irradiation below $\sim 40\text{K}$, the material is converted to a ferromagnetic conductor, and the charge-ordering is destroyed [2]. Simultaneously, substantial changes in the lattice parameters are observed [3]. These changes are associated with the relaxation of the static Jahn-Teller distortion of the Mn^{3+}O_6 octahedra of the CO phase upon the transformation to the metallic phase and the concomitant charge delocalization [2]. However, the depression of the charge-ordering is not observed in all the investigated sample compositions. Therefore, mechanisms of the photoinduced transition which do not depend on the lattice relaxation were proposed [5]. The details of the transition mechanism on a microscopic level are, however, still not completely understood. The nature and the relative importance of the

local electronic and structural changes produced by the photoelectrons in these materials require further investigation. In particular, study of the photoinduced transitions in the manganites exhibiting different properties than those of $\text{Pr}_{1-x}(\text{Ca},\text{Sr})_x\text{MnO}_3$ should be helpful.

In this paper we study $\text{La}_{0.875}\text{Sr}_{0.125}\text{MnO}_3$, a perovskite manganite with a different composition and doping level than the previously investigated Pr-based materials. $\text{La}_{0.875}\text{Sr}_{0.125}\text{MnO}_3$ is orthorhombic at all temperatures. In terms of the underlying distorted primitive cubic perovskite cell dimension a_c , the orthorhombic lattice constants are approximately expressed as $a \sim \sqrt{2}a_c$, $b \sim \sqrt{2}a_c$, $c \sim 2a_c$. The orthorhombic axes a , b , and c run along the $(1\ 1\ 0)_c$, $(1\ -1\ 0)_c$, and $(0\ 0\ 1)_c$ directions in the cubic lattice, respectively. At room temperature, $\text{La}_{0.875}\text{Sr}_{0.125}\text{MnO}_3$ is a semiconductor with the lattice constants satisfying $c/\sqrt{2} \sim a \sim b$ (the O^* phase) [9]. As the temperature is reduced below $T_S \sim 260\text{K}$, it undergoes a transition to the distorted O' phase in which $c/\sqrt{2} < a < b$. At $T_c \sim 190\text{K}$ it becomes a ferromagnetic metal, and finally at $T_{CO} \sim 150\text{K}$ the material undergoes a transition to the charge-ordered canted insulating state which is pseudocubic in analogy to the high-temperature O^* structure [9]. This low temperature state is structurally distinct from the O^* phase [10] and is referred to as the O'' state. The CO state exhibits a static lattice distortion due to the spatial ordering of the Jahn-Teller distorted Mn^{3+}O_6 octahedra. This distortion results in a doubling of the unit cell in the c direction, giving rise to $(H, K, L \pm 0.5)$ neutron diffraction peaks (CO-peaks) [11]. The charge-ordering pattern in $\text{La}_{0.875}\text{Sr}_{0.125}\text{MnO}_3$ is different from the one found in the CO phase of the $\text{Pr}_{1-x}(\text{Ca},\text{Sr})_x\text{MnO}_3$ materials [8].

We find that below $T_x \sim 40\text{K}$ x-rays induce a structural transition at which charge-ordering is destroyed and lattice constants change significantly. As in $\text{Pr}_{0.7}\text{Ca}_{0.3}\text{MnO}_3$, this transition is persistent as evidenced by the fact that the material remains in the x-

ray-converted state when the x-rays are off; however, the CO state can be restored on heating above T_{CO} and subsequent cooling. The low-temperature CO state is possibly metastable below the phase transition temperature T_{S1} , $T_{S1} < 40\text{K}$. The CO-peaks are broad at all temperatures, indicating that the charge-ordered domains never grow larger than $\sim 500\text{\AA}$ in size. Our results show that the photoinduced structural change is a common feature found in the CO phase of the perovskite manganites of various compositions and doping levels.

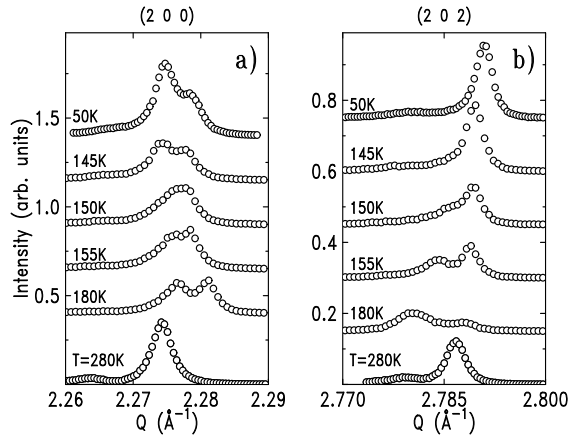


FIG. 1. Longitudinal x-ray diffraction scans in the vicinity of the (2 0 0) and (2 0 2) Bragg peaks at various temperatures.

The measurements were performed in a closed-cycle dispex refrigerator mounted on a four-circle goniometer at beamline X20A at the National Synchrotron Light Source. The x-ray beam was monochromatized by a double crystal Ge (111) monochromator, scattered from the sample, analyzed by the Ge (111) crystal and detected by a scintillation detector. The incident photon energy was 8 keV, and the photon flux was $\sim 3 \times 10^{11}\text{s}^{-1}\text{mm}^{-2}$. Single crystals of $\text{La}_{1-x}\text{Sr}_x\text{MnO}_3$ were grown at MIT by the floating zone technique described elsewhere [12]. The sample composition was verified by electron probe microanalysis. For this experiment, a sample with $x = 0.123 \pm 0.003$ was chosen. The transition temperatures T_S , T_C , and T_{CO} were determined by electrical resistivity and magnetic susceptibility measurements and agreed well with the previously reported values.

To illustrate the structural phase transitions that take place in $\text{La}_{0.875}\text{Sr}_{0.125}\text{MnO}_3$ at T_S and T_{CO} , we show longitudinal (*i.e.* parallel to the scattering vector) x-ray diffraction scans taken at several temperatures in the vicinity of the (2 0 0) and (2 0 2) Bragg peaks in Fig. 1. The orthorhombic structure of $\text{La}_{0.875}\text{Sr}_{0.125}\text{MnO}_3$ is derived from the underlying distorted cubic perovskite structure. Therefore, due to the presence of different twin domains in our sample, (2 0 0), (0 2 0), and (1 1 2) Bragg peaks are simultaneously present in the scans of Fig. 1(a). For the same reason, (2 0 2) and (0 2 2) peaks

are present in Fig. 1(b). A small difference between the a , b , and $c/\sqrt{2}$ lattice constants results in the separation between the Bragg peaks corresponding to different twin domains. The relative intensities of the peaks originating from the different twin domains reflect the relative domain populations in the portion of the sample probed by x-rays. At $T > T_S$, two peaks can be identified in each scan. In Fig. 1(a) the weaker peak is (2 0 0), and the stronger one contains both (0 2 0) and (1 1 2) peaks. In Fig. 1(b), the weaker and the stronger peaks are (2 0 2) and (0 2 2) respectively. The lattice constants obtained from these data are similar to those reported in Refs. [9,10] indicating that the sample is in the O^* phase. At $T_{CO} < T < T_S$ the material is in the distorted O' phase. In this phase, the (2 0 2) and (0 2 2) peaks broaden, indicating that a substantial lattice strain occurs. At $T < T_{CO}$, the material recovers pseudocubic structure [9,10]. This charge-ordered phase, denoted as O'' , is distinct from the high-temperature O^* phase because it exhibits a different type of orthorhombic distortion ($a \gtrsim b \sim c/\sqrt{2}$) [10]. As the result, the diffraction patterns at $T=280\text{K}$ and at $T=50\text{K}$ shown in Fig. 1(a) are clearly different.

We now turn to the x-ray induced structural transition that takes place at $T < T_x \sim 40\text{K}$. Fig. 2(a) shows x-ray diffraction scans in the vicinity of the (2 0 0) Bragg peak at $T=10\text{K}$. The sample was cooled down with no x-rays present. Each scan was taken with the incident x-ray beam attenuated 4000 times to insure that no photoinduced change occurred during the scan. Between the scans, the sample was subjected to the full beam intensity. The total full-beam x-ray exposure time is indicated beside each scan in Fig. 2(a). As the result of the x-ray irradiation, the two diffraction peaks merge. The effects of the x-ray irradiation on the (2 0 2) Bragg peak are shown in Fig. 2(b). No x-ray induced peak broadening is observed in the data of Fig. 2(b), and therefore the crystal lattice long-range order is not affected by the x-rays. The data of Fig. 2(a) were fitted to the sum of two resolution-limited Lorentzian peaks. The results of the fits are shown as solid lines in this figure. The resulting peak separation as a function of x-ray exposure time is shown in Fig. 2(c). Since the peaks are not resolved for times $t > 2\text{ min}$, the peak separation can be smaller than shown in this figure. This is indicated by an extended error bar at $t=30\text{ min}$. The transition is essentially complete after 30 min (5×10^{14} photons per mm^2). In the vicinity of the (2 0 0) and (2 0 2) Bragg positions, the diffraction pattern found in the x-ray converted phase coincides within the accuracy of our experiment with the diffraction pattern found at $T=280\text{K}$, when the latter is corrected for a uniform thermal contraction. This suggests that the x-ray converted phase is similar to the high-temperature O^* phase. However, complete crystal structure determination is required to prove this hypothesis. To sum up, the data of Fig. 2 show that substan-

tial structural changes are induced in $\text{La}_{0.875}\text{Sr}_{0.125}\text{MnO}_3$ when this material is subjected to x-ray irradiation at $T=10\text{K}$. Similar to the case of Pr,Ca-based manganites, the material remains in the x-ray induced state in the absence of x-rays, but the original O'' phase can be restored after heating above T_{CO} and subsequently cooling.

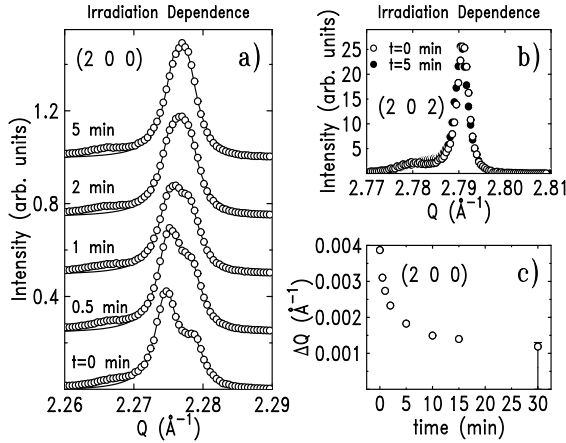


FIG. 2. X-ray irradiation effects on the diffraction scans in the vicinity of a) $(2\ 0\ 0)$, and b) $(2\ 0\ 2)$ Bragg peak positions. The temperature is 10K . The full-beam x-ray exposure time is indicated for each scan. The solid lines in (a) are the results of fits as discussed in the text. Panel (c) shows the peak-separation of (a) as a function of x-ray exposure.

As neutron diffraction measurements of Yamada *et al.* demonstrated [11], charge ordering of Mn^{3+} and Mn^{4+} ions occurs below $T_{CO}=150\text{K}$. The lattice distortion associated with the charge-ordering gives rise to $(H\ K L \pm 0.5)$ diffraction peaks (H, K, L integer). X-ray irradiation has been shown to destroy charge-ordering in $\text{Pr}_{0.7}\text{Ca}_{0.3}\text{MnO}_3$ [2]. The data of Fig. 3 demonstrate that this is also the case for $\text{La}_{0.875}\text{Sr}_{0.125}\text{MnO}_3$. In this figure, the x-ray irradiation dependence of the $(2\ 0\ 1.5)$ CO-peak intensity at $T=10\text{K}$ is shown. The inset in Fig. 3 demonstrates that the structural changes occur only in the presence of x-rays. The CO-peak intensity is reduced by an order of magnitude after 300 min of x-ray exposure. The temperature dependences of the CO-peak intensity and its intrinsic width taken on cooling and on heating are shown in Fig. 4. Due to the weakness of the CO peak, the data had to be taken using the full-beam intensity. The suppression of the CO peak intensity below $T_x=40\text{K}$ is x-ray induced and is not observed in the neutron experiment of Ref. [11]. No x-ray irradiation effects are found for $T > T_x$. The CO-peak intensity does not recover all the way on heating. Instead, it saturates at $T \sim 60\text{K}$. At about the same temperature, the lattice gradually recovers the orthorhombic distortion characteristic to the unexposed material. These data suggest that the CO-state is metastable at low temperatures, with the new equilibrium transition temperature $T_{S1} < 40\text{K}$. A simi-

lar suggestion has been made previously for the case of Pr,Ca-manganites [5]. The CO-peaks are broad at all temperatures, and the correlation length of the charge-ordered state is always smaller than 500\AA . Below T_x , the width of the CO-peaks grows with x-ray exposure. This is illustrated in the bottom panel of Fig. 4: at $T=10\text{K}$, the point with smaller inverse correlation length is taken after 2 hours of x-ray exposure, and the point with larger inverse correlation length – after an additional 9 hours of x-ray irradiation.

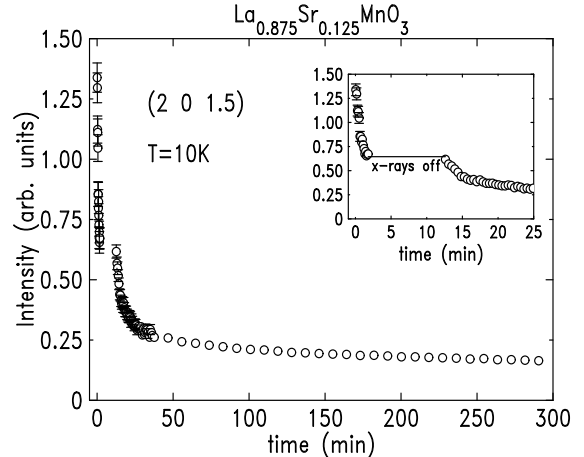


FIG. 3. X-ray irradiation dependence of the $(2\ 0\ 1.5)$ charge-ordering peak intensity at $T=10\text{K}$. The inset shows the CO-peak intensity for $t < 25$ min. The solid line in the inset indicates the period of time when the x-rays were turned off.

The structural changes found in $\text{La}_{0.875}\text{Sr}_{0.125}\text{MnO}_3$ and in $\text{Pr}_{1-x}\text{Ca}_x\text{MnO}_3$ (Refs. [2,3]) are similar. However, the doping level ($x = \frac{1}{8}$), and the CO pattern in $\text{La}_{0.875}\text{Sr}_{0.125}\text{MnO}_3$ are very different from those of Pr,Ca-manganites exhibiting the photoinduced transition. The feature common to the CO phases in manganites is the static ordering of the Jahn-Teller distorted Mn^{3+}O_6 octahedra. The photoinduced relaxation of the lattice distortion associated with this ordering is now found in two different CO systems. This suggests that such a relaxation is an intrinsic feature of the photoinduced transition in manganites. In the model proposed in Ref. [2], an x-ray photon removes an electron from the Jahn-Teller Mn^{3+}O_6 self-trap, leading to the relaxation of the lattice distortion (Mn^{4+} is not a Jahn-Teller ion). The electron goes to the conduction band and is not re-captured because of the metastable nature of either the metallic or the CO state. However, it has been found in more recent work that the structural changes do not always accompany the photoinduced insulator-metal transition [5]. Since the lattice distortion is a characteristic feature of the non-conducting CO state, this result is surprising. However, it can be explained if, as in the case of $\text{Pr}_{0.7}\text{Ca}_{0.3}\text{MnO}_3$, the photoinduced state is highly inho-

mogeneous. It has been shown that in $\text{Pr}_{0.7}\text{Ca}_{0.3}\text{MnO}_3$ the photoinduced transition proceeds via the growth of islands of the second phase inside the original CO phase [3,5]. While the percolating network of such islands results in the insulator-metal transition, the associated lattice relaxation may be unobservable if the fraction of the photoconverted material is small. Thus, one of the possible mechanisms of the x-ray induced transition involves the lattice relaxation caused by the photoelectrons as an essential part. However, other mechanisms have been proposed [5], and more experimental and theoretical work is required to elucidate the microscopic nature of the photoinduced transitions in manganites.

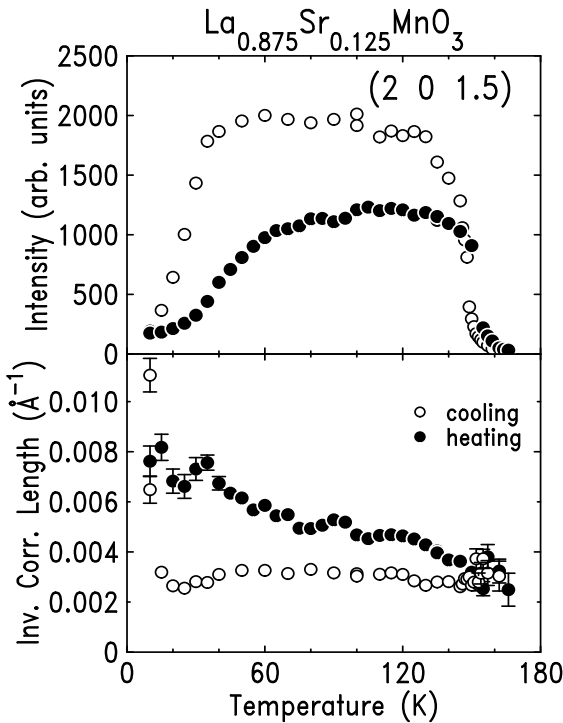


FIG. 4. Temperature dependence of the (2 0 1.5) charge-ordering peak intensity (top panel), and the charge-ordering inverse correlation length (bottom panel) taken on cooling and heating. The correlation length was extracted by fitting the longitudinal x-ray diffraction scans to a Lorentzian fitting function convoluted with the experimental resolution.

Our experiments show no direct evidence of phase separation during the x-ray induced transition. The change of the lattice constants in this transition is relatively small, making observation of the growth of the second phase within the original CO matrix difficult. However, the growth of the CO-peak width with the x-ray exposure is consistent with the gradual diminution of the CO-regions in the course of the transition. In addition, the fact that the characteristic size of the CO regions ($\sim 500\text{\AA}$) is similar to the microdomain size in the phase separated $\text{La}_{0.5}\text{Ca}_{0.5}\text{MnO}_3$ (Ref. [13]) suggests

that the phase separation might already be present in the unexposed material. In both $\text{La}_{1-x}\text{Sr}_x\text{MnO}_3$ and $\text{Pr}_{1-x}\text{Ca}_x\text{MnO}_3$, the CO pattern does not change when the doping level x slightly deviates from the “ideal” commensurate value x_c [7,11] ($x_c = \frac{1}{8}$ for the former, and $x_c = \frac{1}{2}$ for the latter material). The CO phase is most stable at $x = x_c$. In fact, $\text{Pr}_{0.5}\text{Ca}_{0.5}\text{MnO}_3$ undergoes the x-ray induced transition only in high magnetic fields [4]. On the contrary, the transition is easily induced in $\text{La}_{0.875}\text{Sr}_{0.125}\text{MnO}_3$ ($x = x_c$). Without making any statement on the nature of the low-temperature state of this material, we note that the presence of a small O^* phase fraction in the unexposed $\text{La}_{0.875}\text{Sr}_{0.125}\text{MnO}_3$ (phase separation) could explain why this material is so prone to the x-ray induced transition.

The last point that we would like to make is that while the photoinduced transitions found in Pr,Ca-manganites were always of the insulator-metal type, the transport properties of the photoinduced phase in $\text{La}_{0.875}\text{Sr}_{0.125}\text{MnO}_3$ have not yet been determined and will be the subject of future work.

In summary, $\text{La}_{0.875}\text{Sr}_{0.125}\text{MnO}_3$ undergoes an x-ray induced structural transition in which charge ordering of Mn^{3+} and Mn^{4+} ions characteristic to the low-temperature state of this compound is destroyed. The CO phase can be restored by heating above T_{CO} and subsequently cooling. The charge-ordering correlation length is smaller than 500\AA at all temperatures. Together with the recent reports on $\text{Pr}_{1-x}(\text{Ca},\text{Sr})_x\text{MnO}_3$, our results demonstrate that the photoinduced transition is a common property of the charge-ordered perovskite manganites, and that structural changes play an important role in this transition.

This work was supported by the MRSEC Program of the NSF under Award No. DMR 94-00334.

- [1] For a review, see A. P. Ramirez, *J. Phys.: Condens. Matter* **9**, 8171 (1997)
- [2] V. Kiryukhin, D. Casa, J. P. Hill, B. Keimer, A. Vigliante, Y. Tomioka, and Y. Tokura, *Nature (London)* **386**, 813 (1997)
- [3] D. E. Cox, P. G. Radaelli, M. Marezio, S-W. Cheong, *Phys. Rev. B* **57**, 3305 (1998)
- [4] V. Kiryukhin, D. Casa, B. Keimer, J. P. Hill, A. Vigliante, Y. Tomioka, and Y. Tokura, *Mat. Res. Soc. Symp. Proc.* **494**, 65 (1998)
- [5] D. Casa, V. Kiryukhin, O. A. Saleh, B. Keimer, J. P. Hill, Y. Tomioka, and Y. Tokura, preprint cond-mat/9809242
- [6] K. Miyano, T. Tanaka, Y. Tomioka, Y. Tokura, *Phys. Rev. Lett.* **78**, 4257 (1997)
- [7] Y. Tomioka, A. Asamitsu, H. Kuwahara, Y. Moritomo, Y. Tokura, *Phys. Rev. B* **53**, R1689 (1996)

- [8] H. Yoshizawa, H. Kawano, Y. Tomioka, Y. Tokura, *Phys. Rev. B* **52**, R13145 (1995)
- [9] H. Kawano, R. Kajimoto, M. Kubota, H. Yoshizawa, *Phys. Rev. B* **53**, R14709 (1996)
- [10] L. Pinsard, J. Rodriguez-Carvajal, A. H. Moudden, A. Anane, A. Revcolevschi, C. Dupas, *Physica B* **234-236**, 856 (1997)
- [11] Y. Yamada, O. Hino, S. Nohdo, R. Kanao, *Phys. Rev. Lett.* **77**, 904 (1996)
- [12] A. Urushibara, Y. Moritomo, T. Arima, A. Asamitsu, G. Kido, Y. Tokura, *Phys. Rev. B* **51**, 14103 (1995)
- [13] S. Mori, C. H. Chen, S-W. Cheong, *Phys. Rev. Lett.* **81**, 3972 (1998)